Published in final edited form as:
J Immunol. 2011 June 1; 186(11): 6417–6426. doi:10.4049/jimmunol.1001241.

Painful Pathways Induced by Toll-like Receptor Stimulation of Dorsal Root Ganglion Neurons

Jia Qi[*], **Krisztina Buzas**[*,†], **Huiting Fan**[*], **Jeffrey I. Cohen**[‡], **Kening Wang**[‡], **Erik Mont**[§], **Dennis Klinman**[¶], **Joost J. Oppenheim**[*], and **O.M. Zack Howard**[*]

[*] Laboratory of Molecular Immunoregulation, Cancer and Inflammatory Program, Center for Cancer Research, National Cancer Institute-Frederick, MD, USA

[¶] Laboratory of Experimental Immunology, Cancer and Inflammatory Program, Center for Cancer Research, National Cancer Institute-Frederick, MD, USA

[‡] Laboratory of Infectious Diseases, National Institute of Allergy and Infectious Diseases, National Institutes of Health, Bethesda, MD, USA

[§] Nova Scotia Medical Examiner Service, Halifax, Nova Scotia, Canada

Abstract

We hypothesize that innate immune signals from infectious organisms and/or injured tissues may activate peripheral neuronal pain signals. In this study, we demonstrated that toll-like receptors 3/7/9 (TLRs) are expressed by human dorsal root ganglion neurons (DRGNs) and in cultures of primary mouse DRGNs. Stimulation of murine DRGNs with TLR ligands induced expression and production of proinflammatory chemokines and cytokines CCL5 (RANTES), CXCL10 (IP10), interleukin-1alpha, interleukin-1beta, and prostaglandin E2 (PGE_2), which have previously been shown to augment pain. Further, TLR ligands up-regulated the expression of a nociceptive receptor transient receptor potential vanilloid type 1 (TRPV1), and enhanced calcium flux by TRPV1 expressing DRGNs. Using a tumor-induced temperature sensitivity model, we showed that in vivo administration of a TLR9 antagonist, known as a suppressive ODN, blocked tumor-induced temperature sensitivity. Taken together, these data indicate that stimulation of peripheral neurons by TLR ligands can induce nerve pain.

Introduction

Toll-like receptors (TLRs) play a fundamental and essential role in host defense during pathogen infection by regulating and linking innate and adaptive immune responses (1, 2). The twelve mammalian TLRs belong to a family of receptors that recognize pathogen-associated molecular patterns (PAMPs) and can be divided into those that are expressed in the cell membrane and those located in endosomes. The ones located in endosomes, TLR3, TLR7/8 and TLR9 are activated by double stranded and single stranded nucleotides of viral or cellular origin. Innate immune cells sense viral infection by detecting viral proteins and/or nucleic acids. TLR3 is known to be a major mediator of the cellular response to viral infection, because it responds to double-stranded RNA (dsRNA), a common byproduct of

Corresponding author: O. M. Zack Howard, PO Box B, 1050 Boyles St., Frederick MD 21702 (phone) 301 846 1348 (FAX) 301 846 6789, howardz@mail.nih.gov.
[†]Current address Biological Research Centre, Hungarian Academy of Sciences, H-6726 Szeged, Temesvári krt. 62. H-6701 Szeged, P.O. Box 521, Hungary

viral replication (3), whereas, TLR7 and TLR9 are activated by single-stranded RNA (ssRNA) and cytosine-guanosine (CpG) DNA, respectively.

Pain is generated by a combination of sensory and affective components, and classified as physiological, normal or chronic pain. Chronic pain, including tissue injury-associated inflammatory pain and nerve injury-associated neuropathic pain, is often more intense than the underlying tissue damage would predict. The vanilloid receptor one (VR1) which is also known as transient receptor potential vanilloid type 1 (TRPV1), is an ion channel receptor that has been validated as a pain target by chemical stimulation, using capsaicin (CAP) or by endogenous anandamide (Ana), and by genetic deletion (4). Our earlier studies have shown that signals initiated by chemokine receptors (5, 6), which are expressed by both immune and nervous tissue, enhance expression and function of TRPV1 (7). This led us to question if pain sensation in peripheral nervous system neurons could also be enhanced by cross talk between classic innate immune receptors like TLRs and TRPV1.

There is considerable evidence showing that TLRs participate in nerve injury in the peripheral and central nervous systems(8–10), but little evidence showing that neurons respond to innate immune stimuli. TLR3 has a role in the activation of spinal glial cells and the development of tactile allodynia, which is pain in response to inoffensive stimulation after nerve injury(11). Intrathecal administration of TLR3 agonist polyinosine-polycytidylic acid (poly I:C) induced behavioral, morphological, and biochemical changes similar to those observed after nerve injury(11). Conversely, down-regulation of TLR3 inhibited spinal nerve injury induced by pro-inflammatory cytokines, such as interleukin-1beta (IL-1beta), interleukin-6 (IL-6), and tumor necrosis factor-alpha (TNF-alpha) (11). Furthermore, TLR3 antisense oligodeoxynucleotide (ODN) suppressed nerve injury-induced tactile allodynia, and decreased the phosphorylation of p38 mitogen-activated protein kinase (p38 MAPK) in spinal glial cells (11). Lafon et al. reported that human neurons, in the absence of glia, expressed TLR3 and sensed viral dsRNA, thus neurons have the intrinsic machinery to trigger robust inflammatory, chemoattractive, and antiviral responses (12). However, whether TLR3 contributes to pain signals remains unknown. By examining the role of spinal cord glial cells in neuropathic pain and opioid actions, Hutchinson et al. demonstrated that TLR4-dependent glial activation is pivotal to the maintenance of neuropathic pain and TLR4-dependent opioid-induced glial activation is fundamental to reducing morphine analgesia and producing dependence (13). Thus, some TLRs provide a key link between the innate immune system and the nervous system (14–16). This led us to hypothesize that TLR ligands generated by viral infections or cell death may induce painful signals in the peripheral nervous system by stimulating peripheral sensory neurons exemplified by dorsal root ganglion neurons (DRGNs). We therefore investigated whether DRGNs express TLRs and whether the TLRs participate in the pain signals when stimulated by TLR3, 7, or 9 ligands.

In the present study, we demonstrate that both human and mouse DRGNs express TLR3/7/9 and that stimulating mouse DRGNs with TLR3/7/9 ligands increased TLR3/7/9 expression. Murine DRGNs stimulated with TLR ligands increase mRNA expression and protein production of many inflammatory cytokines and chemokines, which have previously been identified as mediators of pain hypersensitivity. Further, TLR ligands up-regulated the expression of TRPV1, a nociceptive receptor and also enhanced calcium (Ca^{2+}) flux mediated by TRPV1. These results provide new insights into the role of TLRs in pain signaling by peripheral neurons.

Material and Methods

Primary DRGN culture

These studies were performed in compliance with the principles and procedures outlined in the National Institutes of Health Guide for the Care and Use f Animals and were approved by the National Cancer Institute Frederick Animal Care and Use Committee (NCI-Frederick, MD, USA) under ASPs 08-005 and 10–218. DRGNs cultures were prepared as described previously (17, 18) with modifications (19). A detailed description of the procedure for the removal of rat DRGs, employed here for both mice and rats, can be found elsewhere (20) as can concerns about plating surface coatings (21). Briefly, DRGs were dissected from 13-day old mouse embryos of NIH Swiss (NIH Swiss is N:NIH(S) which derived from the N:GP(S) colony in 1936), C57BL/6N (NCI Animal Production Program 1999 restart) or MyD88 knock out mice (from Dr. S. Akira further backcrossed to C57BL/6N by Dr. D. Klinman), respectively. 0.05% trypsin-EDTA (Gibco, Carlsbad, CA) was added to the ganglia and incubated at 37 °C for 10 min. After centrifugation at 350 g for 5 min, the cells were resuspended in Dulbecco's Eagle's medium (DMEM) (Mediatech, Herndon, VA) containing 57 °C heat inactivated 10% fetal bovine serum (FBS) (nuclease containing, HyClone, Thermo Scientific, Logan, UT), 4 mM L-glutamine (Quality Biological, Gaithersburg, MD), penicillin-streptomycin (100 units/ml and 100 μg/ml, respectively, Quality Biological, Gaithersburg, MD). The cells (7.5×10^5) were then plated onto 4-well or 8-well chambered coverglass (Nunc, Rochester, NY) pre-coated with poly-L-lysine (Sigma-Aldrich, St. Louis, MO) and collagen type 1 (Inamed Biomaterials, Fremont, CA) for 1 hr. Subsequently, cells were grown in neurobasal medium (Gibco, Carlsbad, CA) supplemented with 10% heat-inactivated horse serum (nuclease containing, Sigma-Aldrich, St. Louis, MO), 2% B-27 supplement (Gibco, Carlsbad, CA), 3 μg/ml glucose, 0.5 μg/ml mitotic inhibitor (Sigma-Aldrich, St. Louis, MO) to inhibit cell division and 100 ng/ml nerve growth factor (NGF) (R&D Systems, Minneapolis, MN) to promote neuronal survival and differentiation. DRGNs cultures were maintained for in the medium in a 5% CO_2 incubator at 37 °C for 4 days, at which point well differentiated dendrites were observed. Primary DRGNs cultures were used on the fifth day of culture.

TLR ligand treatment

TLR ligands, poly I:C (25 μg/ml, TLR3), gardiquimod (3 μg/ml, TLR7 and TLR8) and ODN 1826 (32 μg/ml, TLR9 agonist), ODN 2088 (50 μg/ml, TLR9 antagonist) (InvivoGen, San Diego, CA), were dissolved in media and added to the cultures on day 5 for 16 hrs. Suppressive ODNs for in vivo studies were provided by Dr. Klinman (22, 23). Sup ODN A151 had a phosphorothiate backbone of sequence TTAGGGTTAGGGTTAGGGTTAGGG and was synthesized by the Center for Biologics Evaluation and Research Core Facility

Immunochemistry

Immunochemical analysis was perforxmed on primary cultured embryonic murine DRGNs and adult human DRG sections. Human ganglion were collected at autopsy less than 24 hr after death, frozen on dry ice, and stored at −80°C, before cryostat sections were obtained. The office of human subjects research at NIH deemed this research exempt. Cultured DRGNs and human DRG cryostat sections were fixed with 4 % paraformaldehyde for 10 min, washed with PBS 3 times each for 5 min, permeabilized with 0.1 % Triton X-100 in PBS containing 1 % normal goat serum (NGS) (Sigma-Aldrich, St. Louis, MO) for 10 min, washed with PBS 3 times each for 5 min. Samples were then blocked in 5 % NGS at room temperature for 1 hr. After blocking, the samples were then incubated with primary antibodies, which included rabbit polyclonal antibody against TLR3 (Cat.#3643), TLR7 (Cat.#3269), TLR9 (Cat.#3739) (1:200, respectively, Prosci Inc., Poway, CA, these polyclonal antibodies are mouse and human reactive), TRPV1 (Cat.#NB100-98886,1:1,000,

human and mouse reactive, Novus Biologicals, Littleton, CO) and mouse monoclonal anti-neuron-specific beta-III tubulin (1:200, R&D Systems, Minneapolis, MN) in 2 % NGS overnight at 4 °C. Rabbit IgG (1:200, R&D Systems, Minneapolis, MN) was used as the negative control for TLRs and TRPV1. The samples were then washed with PBS 3 times each for 5 min, and incubated with the appropriate secondary antibodies including Alexa Fluor 546 goat anti-mouse (Invitrogen, Eugene, OR), or Alexa Fluor 488 goat anti-rabbit (Invitrogen, Eugene, OR) at a dilution of 1:1,000 in 2 % NGS in PBS, for 1 hr at room temperature. Samples were then washed with PBS for 3 times each for 5 min and mounted using prolong gold antifade reagent with DAPI (P36935, Invitrogen, Eugene, OR), and examined with a ZEISS LSM 510 laser-scanning microscope (Carl Zeiss MicroImaging Inc., Thornwood, NY) equipped with Argon (excitation 488 nm), DPSS (excitation 561 nm) and Diode (excitation 405 nm) lasers. We used the following procedure to calculate the average intensity of TRPV1 in the neuron surface and dendrites before and after stimulation with TLR ligands. Firstly, we used Otsu's global thresholding algorithm (24) to identify the beta-III tubulin in the red channel. The resulting binary mask of the red channel was then used to calculate the average intensity of TRPV1 in the neuron surface and dendrites (green channel). All image-processing steps were performed using a custom ImageJ (U. S. National Institutes of Health, Bethesda, Maryland, USA, http://rsb.info.nih.gov/ij/) script.

Western blot analysis

DRGNs cultures were lysed in ice cold lysis buffer (62.5 mM Tris-HCl, pH 6.8, 2 % w/v SDS, 10 % glycerol, 50 mM dithiothreitol), briefly sonicated, and centrifuged at 17,000 g at 4 °C for 10 min. Total protein in the supernatant was determined using the BCA Protein assay kit (Pierce, Thermo Scientific, Logan, UT). As a positive control, spleen extract was treated as described above. Equal amounts of protein were subject to electrophoresis on NuPAGE Novex Bis-Tris (Invitrogen, Carlsbad, CA) in 4–12% gradient gels in MOPS buffer, and then transferred to polyvinylidene fluoride (PVDF) membranes (Millipore, Billerica, MA). The membranes were blocked in blocking buffer (TBST: 0.25 M Tris base, 1.37 M NaCl, 0.03 M KCl and 0.1 % Tween 20, pH 7.4, with 5% non-fat milk) at room temperature for 1 hr. The membranes were then incubated with rabbit polyclonal antibody against TLR3, TLR7 and TLR9 (1:1,000, Prosci Inc, Poway, CA), rabbit anti-TRPV1 (1:1,000, Novus Biologicals, Littleton, CO) and rabbit anti-GAPDH (1:1,000, Cat.#2118, Cell Signaling Technology, Danvers, MA) overnight at 4 °C. The blots were washed three times in TBST and incubated with horseradish peroxidase-conjugated anti-rabbit secondary antibody (1:2,000, Cell Signaling Technology, Danvers, MA) for 1 hr at room temperature. Blots were then visualized with enhanced chemiluminescence reagent (GE Healthcare, Pittsburgh, PA).

To quantify Western blot data, developed films were scanned, the immunoreactive bands were digitized, and the densitometry was performed using a custom ImageJ (U. S. National Institutes of Health, Bethesda, Maryland, USA, http://rsb.info.nih.gov/ij/) script. The signal for each lane was calculated by summing the area × intensity of immunoreactivity (gray level of immunoreactive band-background level) of TLR3/7/9 and TRPV1, and normalized with internal control bands (GAPDH). The results, which were presented as mean ± S.E.M., were expressed as percentages of levels in control group (100%) and statistically analyzed with Student's t-test for two-group comparisons. The level of significant was taken as $P < 0.05$. All experiments were performed at least 3 times.

PGE_2 detection

Supernatants from DRGNs cultures, which were pretreated with TLR ligands, poly I:C, gardiquimod, ODN 1826 or ODN 2088 (InvivoGen, San Diego, CA) were collected,

respectively and PGE_2 was detected with PGE_2 EIA (Cayman Chemical, Ann Arbor, MI) as indicated by the manufacturer.

RNA isolation, cDNA synthesis and quantitative real-time PCR array

DRGNs cultures were treated with TLR ligands for 16 hrs. Total RNA was isolated from samples by RT^2 qPCR-Grade™ RNA isolation kit (SABiosciences, Frederick, MD). After checking the purification and quality by nanodrop, RNA was reverse-transcribed into cDNA (PTC-200, MJ Research, Watertown, MA) using the RT^2 first strand kit (SABiosciences, Frederick, MD). Each PCR array for quantitative PCR reaction (mouse Inflammatory Response and Autoimmunity PCR Array, Cat.#PAMM3803, SABioscience, Frederick, MD) was carried out in a 10 μl final volume per well containing cDNA (50 ng) and RT Real-Time SYBR Green/Rox PCR Master Mix (SABioscience, Frederick, MD). Thermal cycling was performed in 384-well format plates using an ABI Prism 7900HT Sequence Detection System (Applied Biosystems, Beverly, MA) according to the manufacturer's instructions. All data were captured using the ABI Prism 7900HT Sequence Detector Software version 2.1 (Applied Biosystems, Beverly, MA) (25) and analyzed by RT^2 Profiler PCR Array Data Analysis software (SABioscience, Frederick, MD).

Cytokine quantification

The expression of selected cytokines, chemokines and their receptors in the supernatant of DRGNs cultures were determined by multiplex array (Aushon Biosystems, Woburn, MA).

Ca^{2+} flux (26)

DRGNs were maintained in 8-well chambered coverglass for 5 days. Time-lapse images (phase contrast) were captured with an Olympus Confocal Laser Scanning Microscope, Fluoview FV1000 (Olympus, Center Valley, PA, equipped with a heated stage maintained at 25 °C and with a constant CO_2 source (5%). For Ca^{2+} imaging, the culture media was removed and DRGNs were washed with Krebs-Ringer solution (124 mM NaCl, 3 mM KCl, 2 mM $CaCl_2$, 2 mM $MgCl_2$, 1.3 mM NaH_2PO_4, 26 mM $NaHCO_3$, 10 mM dextrose, pH=7.4). DRGNs in the coverglass chambers were loaded with Fluo-3 AM (final concentration 5 μM in Krebs-Ringer solution) dissolved in 0.1% dimethyl sulfoxide (DMSO, Sigma-Aldrich, St. Louis, MO) at 37 °C for 30 min. DRGNs were then gently washed using Krebs-Ringer solution to remove free dye. Cultures were illuminated with 488-nm light from a multi Ar+HeNe (Argon and HeNe) laser through an epifluorescence Olympus FV1000 IX81 inverted microscope with a 10 × 0.4 numerical aperture Olympus UPLAPO objective. Light passing through the aperture was filtered by a 505–600 nm band-pass filter (BA505-600). The basal fluorescence level was recorded for 90 seconds just before the application of each reagent. Subsequently, 50 μl CAP (Sigma-Aldrich, Steinheim, Switzerland, final concentration 0.03, 0.1, 1 and 10 μM dissolved in 0.1% DMSO) or Ana (Sigma-Aldrich, St. Louis, MO, final concentration 1.86, 5.57, 16.7 and 50 μM dissolved in 0.1% DMSO) were added for 10 seconds. To confirm the Ca^{2+} flux was mediated by TRPV1, we investigated the effects of SB-366791 (BIOMOL International, Plymouth Meeting, PA), the selective TRPV1 antagonist (27). After being washed following dye Fluo-3 AM loading, the neurons were incubated for 30 min at 25 °C with SB-366791 (1 μM) or without the compound (control). The chambers were then placed onto the microscope plate before the addition of various activators of TRPV1. Images were analyzed for changes in intensity of Ca^{2+}-mediated fluorescence using Fluoview Ver 1.7b software (Olympus, Center Valley, PA) and converted into Rainbow color (26).

Tumor-induced temperature sensitivity

A tumor-induced temperature sensitivity model was adapted to our laboratory from earlier studies (28–30) to investigate whether TLR 9 antagonist (Sup ODN) could decrease temperature sensitivity, which is mediated by TRPV1. This model is considered a neuropathic pain model since the tumor-bearing mice experience temperature hypersensitivity. The model was developed in conjunction with and approved by the National Cancer Institute Frederick Animal Care and Use Committee ASP10-218 (NCI-Frederick, MD). Two million S-180 cancer cells were inoculated into the muscular tissue of female Swiss Webster mice in the immediate vicinity of the sciatic nerve near the trochanter, immediately distal to where the posterior biceps semitendinosus branches off the common sciatic nerve. A negative control group was injected with PBS instead of tumor cells. Paw withdrawal latencies to radiant heat stimulation at 55°C were measured before any procedure and on days 2, 5, 7, 9, 11,13 and 15 after tumor inoculation. Treatment groups consisted of ≥ 8 animals. Suppressive synthetic oligonucleotides (Sup ODN) were delivered ip in a dose range from 5 μg/mouse to 300 μg/mouse (22), the tumor control groups received PBS by ip.

Statistics

Statistical determination of PGE_2 and protein levels in supernatants of DRGNs cultures were performed using Student's t test comparison to control (GraphPad Prism, version 4.0c; GraphPad, San Diego, CA). P values less than 0.05 were considered statistically significant. Data for RNA array were analyzed by RT^2 Profiler PCR Array Data Analysis software (SABioscience, Frederick, MD) and standard deviations calculated as recommended (31). Ca^{2+} responses in activated cells were individually identified and their corresponding to 488 nm emission measured using the Fluoview Ver 1.7b software. Data from activated cells on 8-well coverglass chambers in three dependent experiments (a total of 30 cells) were analyzed in each condition (CAP, Ana only or pretreated with TLR ligands) were obtained, and Ca^{2+} responses (mean of the peak values) were plotted by using Sigmaplot 8.0 software (Fig. 8). The comparison of ligands-induced activation of TRPV1 between non-treated and TLR ligands-pretreated cells was carried out by two-way ANOVA with SPSS Ver 13.0. Linear regression and least squares comparison (GraphPad Prism, version 4.0c; GraphPad, San Diego, CA) were utilized to determine the slope and correlation within treatment groups and one-way ANOVA with post tests used to determine the probability and dosing trend.

Results

TLR3/7/9 expressed by DRGNs

In order to show that DRGNs express TLR3/7/9 we established primary cultures from day 13 mouse embryos. In these cultures, greater than ninety five percent of the cells showed phenotypic properties of neurons (32, 33). Immunofluorescence staining on day 5 showed that TLR3, TLR7 or TLR9, which are pseudo-colored green in the micrographs, are expressed on neurons isolated from DRGs (Fig. 1A, 1B and 1C, respectively). Immunofluorescent controls are shown in Fig. 3A. We also found that TLR3, 7 and 9 were expressed by neurons in adult human DRG tissue sections (Fig. 2A, 2B and 2C, negative controls shown in Fig. 3B and 3C). Beta-III tubulin, which is a neuron specific marker, is pseudo-colored red in the micrographs, verified that the cells expressing TLRs were neurons.

TLR ligands enhanced TLR3/7/9 expression by DRGNs

Based on our pilot studies (reported at the NIH-Immunology Interest Group retreat in 2007, Virginia), we determined the optimal nontoxic dose of stimulants to be 25 μg/ml poly I:C, 3

μg/ml gardiquimod or 32 μg/ml ODN 1826 over a 16 hrs incubation period. We applied these individual treatments to determine if DRGNs could respond to TLR ligand stimulation. Western blotting analysis indicated that incubation with the ligands promoted TLR3/7/9 expression (Fig. 4A, 4B and 4C). Spleen lysate was used as the positive control to confirm the expression of TLR3 (~105 kDa), TLR7 (~140 kDa) and TLR9 (~95 kDa). Densitometry results are shown in Fig. 4D.

TLR3/7/9 ligands stimulated prostaglandin E2 (PGE_2) release by mouse DRGNs cultures

PGE_2 is a central mediator of febrile response triggered by the inflammatory process and intradermal PGE_2 is hyperalgesic in the peripheral nervous system (34, 35). We determined the PGE_2 levels in the supernatants of 5-day DRGNs cultures following stimulation for 16 hrs. As shown in Fig. 5A, PGE_2 concentration increased after stimulation by each of the TLR3/7/9 ligands compared with control group ($P < 0.005$), which suggests that ligands for endosomal TLRs could induce DRGNs to produce this mediator of hyperalgesia and inflammation, namely PGE_2. Moreover, we found that ODN 2088 (50 μg/ml), which is an antagonist of TLR9, reduced PGE_2 levels induced by ODN 1826 (32 μg/ml) by 31.8% compared with ODN 1826 alone of maximum stimulation ($P = 0.009$). We also determined the PGE_2 concentration in the supernatants of DRGNs cultures of MyD88 knock out mice. As shown in Fig. 5B, gardiquimod and ODN 1826 failed to induce PGE_2 production significantly in MyD88 KO mice ($P < 0.01$), but as anticipated poly I:C did induce PGE_2 in the knockout DRGN.

TLR ligands up-regulated mRNA levels and protein expression of proinflammatory cytokines and chemokines by DRGNs

To confirm that ligands of endosomal TLRs induce a proinflammatory response by DRGNs, we performed real-time qPCR (mouse Inflammatory Response and Autoimmunity PCR Array) to analyze mRNA levels in DRGNs following stimulation for 16 hrs with poly I:C, gardiquimod or ODN 1826, respectively. TLR ligands dramatically increased the mRNA levels of CCL5, CXCL10, IL-1alpha and IL-1beta (Table 1), which were previously identified as important mediators of the pain hypersensitivity (5–7, 36, 37). Furthermore, as shown in Table 1., TLR3/7/9 ligands also increased IL-1alpha and IL-1beta protein production. Moreover, poly I:C increased CXCL10 and CCL5 protein production, markedly. These data indicate that DRGNs respond to ligands of endosomal TLRs by producing high levels of proinflammatory mediators.

TLR ligands increased TRPV1 expression and translocation by DRGNs

The effect of TLR stimulation on TRPV1, the pain detector and integrator, was evaluated. As shown in Fig. 6, TLR ligands markedly increased TRPV1 (~100 kDa) expression by DRGNs. Moreover, TLR ligands enhanced translocation of TRPV1 proteins from cell bodies in DRGNs to sensory nerve endings (Fig. 7). The elevated TRPV1 expression and translocation suggested that the nociceptive neurons stimulated by TLR ligands are better able to respond to pain stimuli. We next evaluated an in vitro correlate for pain sensation, calcium flux.

TLR ligands enhanced Ca^{2+} influx induced by CAP and Ana

For studies of Ca^{2+} influx, neurons were maintained in culture for 5 days and only small to medium size neurons were studied. Murine DRGNs responded with a persistent and concentration-dependent increase in Ca^{2+} influx following stimulation with CAP as indicated by an increase in the fluorescence intensity of Fluo-3 emission at 488 nm excitation (Fig. 8). This demonstrated that TRPV1 in primary cultured DRGNs were functional. As shown in Fig. 8A, DRGNs responded to 0.1 μM CAP with a much greater

change in fluorescence intensity when pretreated with poly I:C, gardiquimod or ODN 1826 for 16 hrs at 37 °C. Also, activation of TLR3, TLR7 or TLR9 resulted in marked increases in the sensitivity of TRPV1 to various concentrations of CAP (0.03, 0.1 and 1 μM) (Fig. 8B) ($P = 0.008$, $P = 0.039$, and $P = 0.041$, respectively). We further confirmed the enhanced sensitization of TRPV1 induced by TLR ligands by using an endogenous ligand of TRPV1, Ana. DRGNs consistently responded to Ana with an enhanced Ca^{2+} influx when pretreated with poly I:C, gardiquimod or ODN 1826 (Fig. 8C). The Ca^{2+} influx in neurons pretreated with TLR ligands was higher in the presence of 1.86, 5.57 or 16.7 μM Ana (Fig. 8C) (poly I:C $P = 0.009$, gardiquimod $P = 0.029$ or ODN 1826 $P = 0.048$). The Ca^{2+} influx induced by CAP in DRGNs was totally blocked by SB-366791 (Fig. S1), a selective TRPV1 antagonist. Conversely, no Ca^{2+} influx in DRGNs was observed when TLR ligands alone were applied (Fig. S2). These studies show that in addition to inducing the production of inflammatory pain inducing mediators, TLR ligands also up-regulated expression of functional TRPV1 pain signaling receptors.

Suppressive ODN treatment blocks tumor-induced pain sensitivity

Suppressive oligonucleotides, which mimic the suppressive effect of self-DNA by decreasing the immune activating signals of TLR9, were tested in a mouse model of tumor-induce neuropathic pain for their ability to decrease temperature sensitivity. As can be seen in Fig. 9, fibrosarcoma tumor cells implanted near the sciatic nerve result in decreased time of paw withdrawal, indicating hypersensitive to heat in the tumor-bearing mice. When compared to negative control or naïve mice, the tumor-bearing mice show a significantly faster withdrawal from the hot plate that increases over time ($P<0.001$). We were unable to evaluate longer time points because tumor-bearing mice begin to show stress by day 15 and must be euthanized. Treating the tumor-bearing mice with suppressive oligonucleotides, which block TLR9-mediated immune stimulation, resulted in an increase in time of paw withdrawal from the heat challenge, indicating a reduction in heat sensitivity. Fig. 9 shows a dose response from no treatment to 320 μg/mouse of Sup ODN. Beginning at the 20 μg/mouse dose, the difference between the negative control and the tumor-bearing and treated groups become suppressed, indicating that treatment with Sup ODN reduced tumor-induced pain. The reduction in heat sensitivity becomes significant at the 80 μg/mouse dose. This was not due to inhibition of tumor growth because a reduction in tumor growth was not observed until the highest tolerated dose (320 μg/mouse) of Sup ODN (data not shown). The paw withdrawal latencies for naïve mice receiving 320 μg/mouse Sup ODN were not significantly different from control group (data not shown). Thus, our data indicates that suppression of TLR9 leads to reduced sensitivity to heat in a neuropathic pain model despite the presence of a growing tumor, when the suppressive oligonucleotides are delivered outside of the CNS. Taken together, our observations suggest a connection between suppression of a heat activated pain receptor in the peripheral nervous system, when a mouse is treated with a suppressive TLR9 oligonucleotide.

Discussion

One of the cardinal signals of inflammation is pain. Pathogens, injury and stressors stimulate TLRs on innate immune cells thereby initiating the pro-inflammatory signal-transduction pathways that ultimately trigger cytokine production. In the present study, we find that TLRs, which are also expressed by peripheral neuronal cells in response to synthetic ligands produce cytokines and chemokines protein products, such as IL-1alpha, IL-1beta, RANTES and IP10, which have previously been shown to act as pain mediators (5, 6, 36–38).

The present results provide evidence, for the first time, that primary cultured mouse DRGNs constitutively express TLR3/7/9 and respond to their ligands. We focused on embryonic DRGNs because the resulting cultures generate highly pure (>95%) single neurons, thereby

allowing us to selectively investigate neuronal TLR expression and responsiveness to TLR ligands. Our results indicate that DRGNs have the potential to recognize viral and cellular products and initiate an inflammatory response in the peripheral nervous system (PNS) without prior activation of immune cells to produce proinflammatory cytokines. Indeed, in our study, stimulation by the TLR ligands (poly I:C, gardiquimod and ODN 1826) induced cytokines (IL-1alpha and IL-1beta) and chemokine (CCL5 and CXCL10) gene expression and protein production by DRGNs. Moreover, the activation of TLRs produced PGE_2, which acts as a pain inducer. TLR ligand stimulation also enhanced expression and translocation of TRPV1. Furthermore, TRPV1 relocated from the DRGN cell bodies into dendrites following TLR ligand stimulation. TPRV1 relocalization has been reported to be involved in the development of hyperalgesia *in vivo* (39, 40). Notably, pretreatment with TLR ligands also enhanced the TRPV1-mediated Ca^{2+} flux induced by CAP in DRGNs. Thus, peripheral neurons function to bridge the innate immune and sensory systems.

Previous studies demonstrated that TLRs are widely expressed in the central nervous system, particularly by microglia (41). Activation of TLRs on microglia and astrocytes leads to production of cytokines, cellular adhesion molecules, chemokines, and the expression of surface antigens that results in a nervous system immune cascade. Therefore, TLRs also invoke inflammation in the nervous system (42, 43). TLRs expressed on microglia appear to trigger microglial activation, which might be a driving force of chronic pain. Acosta et al. have shown that lipopolysaccharide (LPS), by stimulating TLR4, regulates the expression of the peptide nociceptin/orphanin FQ (N/OFQ), which contributes to feeding behavior. These observations show that TLR4 potentially acts as a key initiator of behavioral responses mediated by DRGNs (44). In addition, immunohistochemical analysis of human and rat trigeminal neurons demonstrated that capsaicin-sensitive nociceptors express TLR4, thus enabling sensory neurons to respond to tissue levels of bacterial substances such as LPS (45).

Other cells in the PNS, including Schwann cells, respond to TLR ligands by producing proinflammatory factors. Poly I:C is responsible for stimulating inducible nitric oxide synthase (iNOS) gene expression and nitric oxide (NO) production in Schwann cells, which exerts neurotoxic effects on DRGNs (46). Our results confirm and extend earlier observations that TLR3/7/9 are expressed by DRGNs (47). Our studies demonstrate that DRGNs respond to the TLR ligand stimulation, indicating that they are functional and suggests that DRGNs through their response to TLR ligands mediate neuronal function.

Ca^{2+} influx induced by TRPV1 activation is one of the causes of pain perception in the nervous system(48). We observed Ca^{2+} influx in DRGNs following stimulation with CAP or Ana, which indicates that the primary cultured DRGNs respond to TRPV1 ligands. SB-366791, a selective TRPV1 antagonist, totally blocked Ca^{2+} influx, suggesting that Ca^{2+} influx was mediated by TRPV1. A dramatic increase in Ca^{2+} was observed in DRGNs after pretreatment with TLR ligands. Therefore, TLR ligands not only up-regulated TRPV1 expression, but also enhanced its activity. At the same time, Ca^{2+} influx through TRPV1 in the nociceptive neuron endings is known to cause the release of mediators of inflammation such as substance P (SP) and calcitonin gene-related peptide (CGRP). SP and CGRP synergize to induce a phenomenon called neurogenic inflammation that results in increased blood-brain barrier permeability (49). Investigating the effect of delivering TLR agonists to the PNS on the blood-brain barrier permeability will require future in vivo studies.

Inflammation induces neuropathic pain, which is experienced as hypersensitivity to thermal, mechanical or chemical stimuli. The model of neuropathic pain used in this study, implantation of fibrosarcoma S-180 cells near the sciatic nerve, is thought to induce pain through two pathways, mechanical restriction of the nerve (28) as the tumor grows and

tumor produced soluble factors like PGE_2 (50), and chemokines (51). Here we have shown that suppressive oligonucleotides that block TLR9-mediated immune activation (22), also block sensitivity to heat which is thought to be mediated by TRPV1(52). Taken with our in vitro data this in vivo data indicates that there is functional cross talk between innate immune receptors (TLRs) and pain sensory receptors (TRPV) in peripheral neurons.

In summary, our findings provide an intriguing example of a set of receptors shared between cells of the immune and the nervous systems that are likely to enhance the responses of both systems. These studies show that TLRs have the potential to have both direct and indirect effects on pain initiation and regulation. Therefore, DRGNs and TLRs are likely to be important contributors to chronic pain and a rewarding target in the development of novel therapeutic strategies in the prevention development and reduction of chronic pain.

Supplementary Material

Refer to Web version on PubMed Central for supplementary material.

Acknowledgments

This study was supported by the intramural research programs of the National Cancer Institute and the National Institute of Allergy and Infectious Diseases.

We would like to thank Drs Emilia Madarasz and R. Douglas Fields for sharing their neuron culture conditions and providing hands on training. We would like to thank our animal technician, Steve Stull, for invaluable support.

References

1. Marshak-Rothstein A. Toll-like receptors in systemic autoimmune disease. Nat Rev Immunol. 2006; 6:823–835. [PubMed: 17063184]
2. Busconi L, Lau CM, Tabor AS, Uccellini MB, Ruhe Z, Akira S, Viglianti GA, Rifkin IR, Marshak-Rothstein A. DNA and RNA autoantigens as autoadjuvants. J Endotoxin Res. 2006; 12:379–384. [PubMed: 17254393]
3. Jacobs BL, Langland JO. When two strands are better than one: the mediators and modulators of the cellular responses to double-stranded RNA. Virology. 1996; 219:339–349. [PubMed: 8638399]
4. Cortright DN, Szallasi A. TRP channels and pain. Curr Pharm Des. 2009; 15:1736–1749. [PubMed: 19442187]
5. Gosselin RD, Dansereau MA, Pohl M, Kitabgi P, Beaudet N, Sarret P, Melik Parsadaniantz S. Chemokine network in the nervous system: a new target for pain relief. Curr Med Chem. 2008; 15:2866–2875. [PubMed: 18991641]
6. Abbadie C. Chemokines, chemokine receptors and pain. Trends Immunol. 2005; 26:529–534. [PubMed: 16099720]
7. Zhang N, Inan S, Cowan A, Sun R, Wang JM, Rogers TJ, Caterina M, Oppenheim JJ. A proinflammatory chemokine, CCL3, sensitizes the heat- and capsaicin-gated ion channel TRPV1. Proc Natl Acad Sci U S A. 2005; 102:4536–4541. [PubMed: 15764707]
8. Downes CE, Crack PJ. Neural injury following stroke: are Toll-like receptors the link between the immune system and the CNS? Br J Pharmacol. 2010; 160:1872–1888. [PubMed: 20649586]
9. Lehnardt S. Innate immunity and neuroinflammation in the CNS: the role of microglia in Toll-like receptor-mediated neuronal injury. Glia. 2010; 58:253–263. [PubMed: 19705460]
10. Lehnardt S, Lehmann S, Kaul D, Tschimmel K, Hoffmann O, Cho S, Krueger C, Nitsch R, Meisel A, Weber JR. Toll-like receptor 2 mediates CNS injury in focal cerebral ischemia. J Neuroimmunol. 2007; 190:28–33. [PubMed: 17854911]
11. Obata K, Katsura H, Miyoshi K, Kondo T, Yamanaka H, Kobayashi K, Dai Y, Fukuoka T, Akira S, Noguchi K. Toll-like receptor 3 contributes to spinal glial activation and tactile allodynia after nerve injury. J Neurochem. 2008; 105:2249–2259. [PubMed: 18363823]

12. Lafon M, Megret F, Lafage M, Prehaud C. The innate immune facet of brain: human neurons express TLR-3 and sense viral dsRNA. J Mol Neurosci. 2006; 29:185–194. [PubMed: 17085778]
13. Hutchinson MR, Zhang Y, Brown K, Coats BD, Shridhar M, Sholar PW, Patel SJ, Crysdale NY, Harrison JA, Maier SF, Rice KC, Watkins LR. Non-stereoselective reversal of neuropathic pain by naloxone and naltrexone: involvement of toll-like receptor 4 (TLR4). Eur J Neurosci. 2008; 28:20–29. [PubMed: 18662331]
14. Olson JK, Miller SD. Microglia initiate central nervous system innate and adaptive immune responses through multiple TLRs. J Immunol. 2004; 173:3916–3924. [PubMed: 15356140]
15. Kalmar B, Kittel A, Lemmens R, Kornyei Z, Madarasz E. Cultured astrocytes react to LPS with increased cyclooxygenase activity and phagocytosis. Neurochem Int. 2001; 38:453–461. [PubMed: 11222926]
16. DeLeo JA, Tanga FY, Tawfik VL. Neuroimmune activation and neuroinflammation in chronic pain and opioid tolerance/hyperalgesia. Neuroscientist. 2004; 10:40–52. [PubMed: 14987447]
17. Zhang PL, Levy AM, Ben-Simchon L, Haggiag S, Chebath J, Revel M. Induction of neuronal and myelin-related gene expression by IL-6-receptor/IL-6: a study on embryonic dorsal root ganglia cells and isolated Schwann cells. Exp Neurol. 2007; 208:285–296. [PubMed: 17963753]
18. Paivalainen S, Nissinen M, Honkanen H, Lahti O, Kangas SM, Peltonen J, Peltonen S, Heape AM. Myelination in mouse dorsal root ganglion/Schwann cell cocultures. Mol Cell Neurosci. 2008; 37:568–578. [PubMed: 18206387]
19. Varga BV, Hadinger N, Gocza E, Dulberg V, Demeter K, Madarasz E, Herberth B. Generation of diverse neuronal subtypes in cloned populations of stem-like cells. BMC Dev Biol. 2008; 8:89. [PubMed: 18808670]
20. Kleitman, N.; Wood, PM.; Bunge, RP. Tissue culture methods for the study of myelination. Oxford University Press; New York: 1997.
21. Okun E, Mattson MP. Phosphothioated oligodeoxynucleotides induce nonspecific effects on neuronal cell adhesion in a growth substrate-dependent manner. J Neurosci Res. 2009; 87:1947–1952. [PubMed: 19156868]
22. Klinman D, Shirota H, Tross D, Sato T, Klaschik S. Synthetic oligonucleotides as modulators of inflammation. J Leukoc Biol. 2008; 84:958–964. [PubMed: 18430787]
23. Dong L, Ito S, Ishii KJ, Klinman DM. Suppressive oligodeoxynucleotides delay the onset of glomerulonephritis and prolong survival in lupus-prone NZB x NZW mice. Arthritis Rheum. 2005; 52:651–658. [PubMed: 15692999]
24. Otsu N. A threshold selection method from gray level. IEEE Trans Systems, Man an dCybernetics. 1979; 9:62–66.
25. Scuto A, Kirschbaum M, Kowolik C, Kretzner L, Juhasz A, Atadja P, Pullarkat V, Bhatia R, Forman S, Yen Y, Jove R. The novel histone deacetylase inhibitor, LBH589, induces expression of DNA damage response genes and apoptosis in Ph- acute lymphoblastic leukemia cells. Blood. 2008; 111:5093–5100. [PubMed: 18349321]
26. Birch BD, Eng DL, Kocsis JD. Intranuclear Ca2+ transients during neurite regeneration of an adult mammalian neuron. Proc Natl Acad Sci U S A. 1992; 89:7978–7982. [PubMed: 1518824]
27. Gunthorpe MJ, Rami HK, Jerman JC, Smart D, Gill CH, Soffin EM, Luis Hannan S, Lappin SC, Egerton J, Smith GD, Worby A, Howett L, Owen D, Nasir S, Davies CH, Thompson M, Wyman PA, Randall AD, Davis JB. Identification and characterisation of SB-366791, a potent and selective vanilloid receptor (VR1/TRPV1) antagonist. Neuropharmacology. 2004; 46:133–149. [PubMed: 14654105]
28. Lee HJ, Lee JH, Lee EO, Kim KH, Kim SH, Lee KS, Jung HJ. Substance P and beta-endorphin mediate electro-acupuncture induced analgesia in mouse cancer pain model. J Exp Clin Cancer Res. 2009; 28:102. [PubMed: 19607689]
29. Shimoyama M, Tanaka K, Hasue F, Shimoyama N. A mouse model of neuropathic cancer pain. Pain. 2002; 99:167–174. [PubMed: 12237194]
30. Asai H, Ozaki N, Shinoda M, Nagamine K, Tohnai I, Ueda M, Sugiura Y. Heat and mechanical hyperalgesia in mice model of cancer pain. Pain. 2005; 117:19–29. [PubMed: 16043290]
31. Cumming G, Fidler F, Vaux DL. Error bars in experimental biology. J Cell Biol. 2007; 177:7–11. [PubMed: 17420288]

32. Itoh K, Stevens B, Schachner M, Fields RD. Regulated expression of the neural cell adhesion molecule L1 by specific patterns of neural impulses. Science. 1995; 270:1369–1372. [PubMed: 7481827]
33. Itoh K, Ozaki M, Stevens B, Fields RD. Activity-dependent regulation of N-cadherin in DRG neurons: differential regulation of N-cadherin, NCAM, and L1 by distinct patterns of action potentials. J Neurobiol. 1997; 33:735–748. [PubMed: 9369148]
34. Heinricher MM, Neubert MJ, Martenson ME, Goncalves L. Prostaglandin E2 in the medial preoptic area produces hyperalgesia and activates pain-modulating circuitry in the rostral ventromedial medulla. Neuroscience. 2004; 128:389–398. [PubMed: 15350650]
35. Summer GJ, Dina OA, Levine JD. Enhanced inflammatory hyperalgesia after recovery from burn injury. Burns. 2007; 33:1021–1026. [PubMed: 17707592]
36. Bhangoo S, Ren D, Miller RJ, Henry KJ, Lineswala J, Hamdouchi C, Li B, Monahan PE, Chan DM, Ripsch MS, White FA. Delayed functional expression of neuronal chemokine receptors following focal nerve demyelination in the rat: a mechanism for the development of chronic sensitization of peripheral nociceptors. Mol Pain. 2007; 3:38. [PubMed: 18076762]
37. Benamar K, Geller EB, Adler MW. Elevated level of the proinflammatory chemokine, RANTES/CCL5, in the periaqueductal grey causes hyperalgesia in rats. Eur J Pharmacol. 2008; 592:93–95. [PubMed: 18656466]
38. Prehaud C, Megret F, Lafage M, Lafon M. Virus infection switches TLR-3-positive human neurons to become strong producers of beta interferon. J Virol. 2005; 79:12893–12904. [PubMed: 16188991]
39. Ji RR, Samad TA, Jin SX, Schmoll R, Woolf CJ. p38 MAPK activation by NGF in primary sensory neurons after inflammation increases TRPV1 levels and maintains heat hyperalgesia. Neuron. 2002; 36:57–68. [PubMed: 12367506]
40. Sibley, DR.; Hanin, I.; Kuhar, M.; Skolnick, P., editors. Handbook of Contempory Neuorpharmacology. Wiley-Interscience; 2007. Handbook of Contempory Neuorpharmacology; p. 729
41. Kielian T. Toll-like receptors in central nervous system glial inflammation and homeostasis. J Neurosci Res. 2006; 83:711–730. [PubMed: 16541438]
42. Pedras-Vasconcelos J, Puig M, Verthelyi D. TLRs as therapeutic targets in CNS inflammation and infection. Front Biosci (Elite Ed). 2009; 1:476–487. [PubMed: 19482661]
43. Wang H, Zhou M, Brand J, Huang L. Inflammation and taste disorders: mechanisms in taste buds. Ann N Y Acad Sci. 2009; 1170:596–603. [PubMed: 19686199]
44. Acosta C, Davies A. Bacterial lipopolysaccharide regulates nociceptin expression in sensory neurons. Journal of Neuroscience Research. 2008; 86:1077–1086. [PubMed: 18027846]
45. Wadachi R, Hargreaves KM. Trigeminal nociceptors express TLR-4 and CD14: a mechanism for pain due to infection. J Dent Res. 2006; 85:49–53. [PubMed: 16373680]
46. Lee H, Park C, Cho IH, Kim HY, Jo EK, Lee S, Kho HS, Choi SY, Oh SB, Park K, Kim JS, Lee SJ. Double-stranded RNA induces iNOS gene expression in Schwann cells, sensory neuronal death, and peripheral nerve demyelination. Glia. 2007; 55:712–722. [PubMed: 17348024]
47. Barajon I, Serrao G, Arnaboldi F, Opizzi E, Ripamonti G, Balsari A, Rumio C. Toll-like receptors 3, 4, and 7 are expressed in the enteric nervous system and dorsal root ganglia. J Histochem Cytochem. 2009; 57:1013–1023. [PubMed: 19546475]
48. Baron R. Neuropathic pain: a clinical perspective. Handb Exp Pharmacol. 2009:3–30. [PubMed: 19655103]
49. Donkin JJ, Vink R. Mechanisms of cerebral edema in traumatic brain injury: therapeutic developments. Curr Opin Neurol. 2010; 23:293–299. [PubMed: 20168229]
50. DeGowin RL, Gibson DP. Prostaglandin-mediated enhancement of erythroid colonies by marrow stromal cells (MSC). Exp Hematol. 1981; 9:274–280. [PubMed: 7227477]
51. Khasabova IA, Stucky CL, Harding-Rose C, Eikmeier L, Beitz AJ, Coicou LG, Hanson AE, Simone DA, Seybold VS. Chemical interactions between fibrosarcoma cancer cells and sensory neurons contribute to cancer pain. J Neurosci. 2007; 27:10289–10298. [PubMed: 17881535]

52. Rau KK, Jiang N, Johnson RD, Cooper BY. Heat sensitization in skin and muscle nociceptors expressing distinct combinations of TRPV1 and TRPV2 protein. J Neurophysiol. 2007; 97:2651–2662. [PubMed: 17287441]

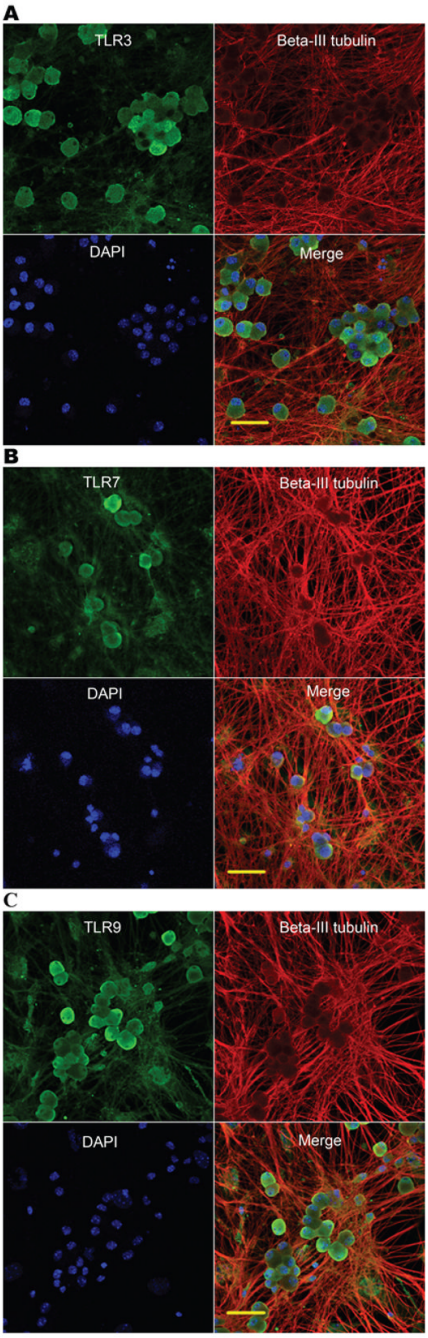

Fig. 1.

DRGNs express TLR3, TLR7 and TLR9. Confocal images of primary cultured mouse DRGNs isolated from E13 embryos are shown. DRGNs were stained with TLR3 (A), TLR7 (B) and TLR9 (C) (green), neuron-specific beta-III tubulin (red) and DAPI (blue). Shown are separate monochrome images of the green, red and blue fluorescence channel, and merged color images from all channels. Scale bars: 50 μm.

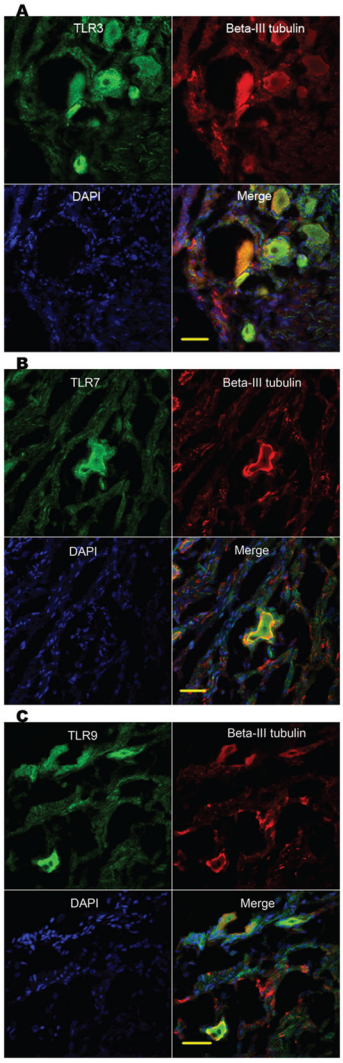

Fig. 2.

Human DRG sections express TLR3, TLR7 and TLR9. Confocal images of DRG cryostat sections. Samples were stained with TLR3 (A), TLR7 (B) and TLR9 (C) (green), neuron-specific beta-III tubulin (red) and DAPI (blue). Shown are separate monochrome images of the green, red and blue fluorescence channel, and merged color images from all channels. Scale bars: 50 μm.

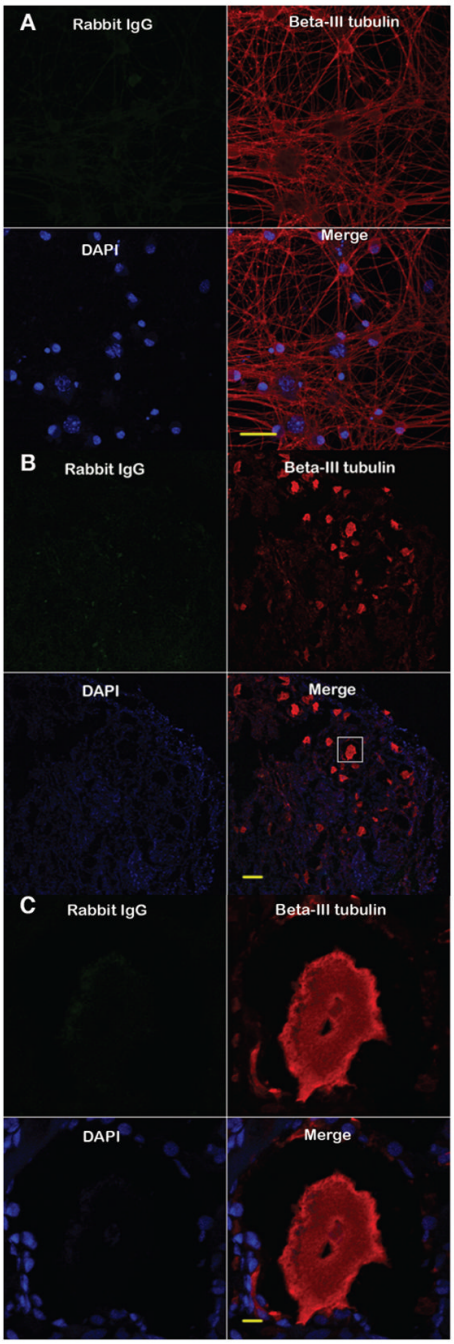

Fig. 3.

Negative control staining for TLRs and TRPV1 in DRGNs (A), TRPV1 in human DRGNs sections (B), and magnified images from human sections (C). Scale bars: 50 μm, 100 μm, and 10 μm, respectively.

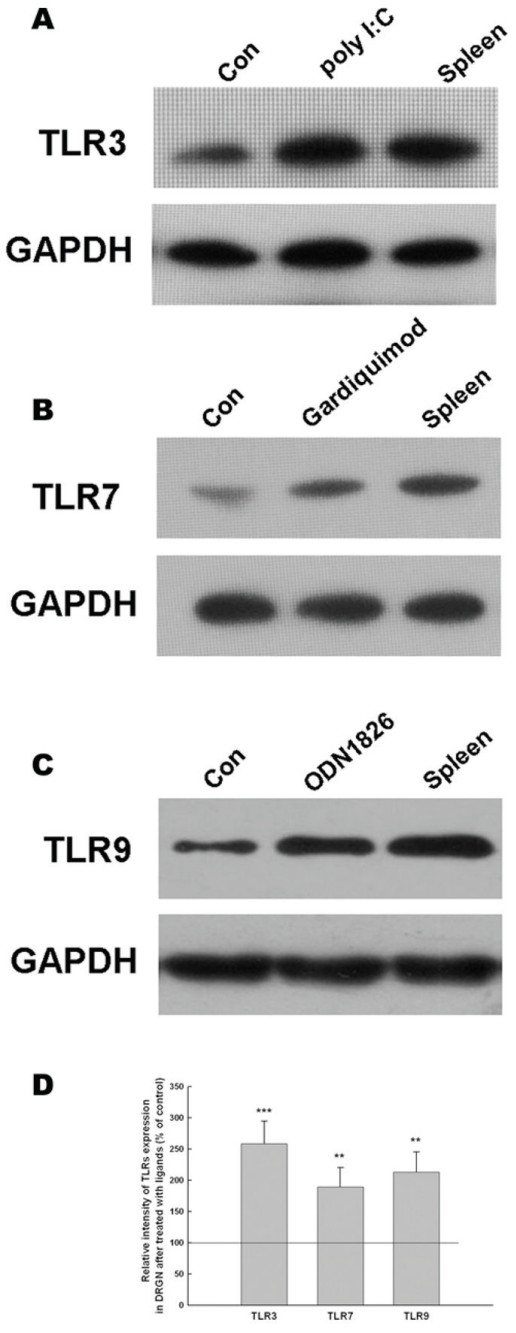

Fig. 4.

TLR ligands induce corresponding receptor expression by DRGNs. Western blot showing TLR3, TLR7 and TLR9 expression by DRGNs following ligand stimulation are shown. (A) poly I:C (25 μg/ml) induced TLR3 protein expression, (B) gardiquimod (3 μg/ml) induced TLR7 protein expression, and (C) ODN 1826 (32 μg/ml) induced TLR9 expression in DRGNs. (D) Densitometry from the blots. Cells were stimulated for 16 hrs then harvested, lysed, and the protein extracts were probed with anti-TLR3, anti-TLR7, and anti-TLR9 antibody. Control (Con) samples were cultured for 16 hrs without additional stimulation. Protein loading is reported using an anti-GPDH antibody. Spleen lysate was used as a positive control. One representative of more than three independent experiments is shown.

Image densitometry were performed using ImageJ software. The densitometry results were determined for 5 sites within each band, presented as mean ± S.E.M., are expressed as percentages of levels in control group (100%). GAPDH was utilized as internal control. Statistics analysis was performed using Student's t test for two-group comparisons. $^{**}P < 0.01$, $^{***}P < 0.001$ compared with control.

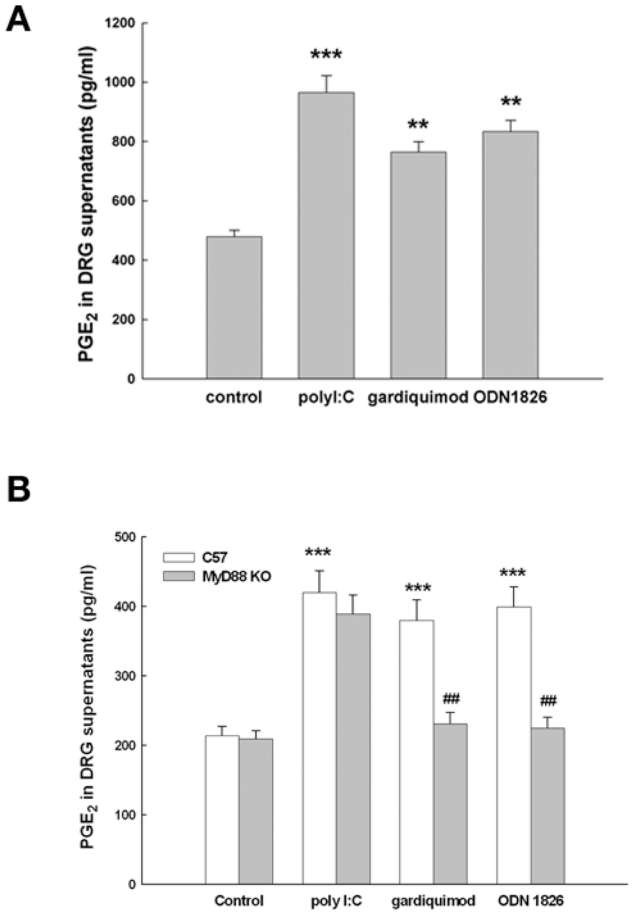

Fig. 5.

TLR ligands induce PGE_2 production by DRGNs. Supernatants of DRGNs cultures were collected and PGE_2 was detected using EIA following stimulation by poly I:C (25 μg/ml), gardiquimod (3 μg/ml) or ODN 1826 (32 μg/ml) for 16 hrs. Each bar represents the mean ± S.E.M. (n=10). (A) PGE_2 production by DRGNs from Swiss embryonic mice, and (B) PGE_2 production by DRGNs from C57 and MyD88 knock out embryonic mice. $^{**}P$ <0.01, $^{***}P$ <0.001 compared with corresponding control, $^{\#\#}P$ <0.01 compared with corresponding C57 mice treated with gardiquimod and ODN 1826. Statistical analysis was performed using Student's t test for two-group comparisons.

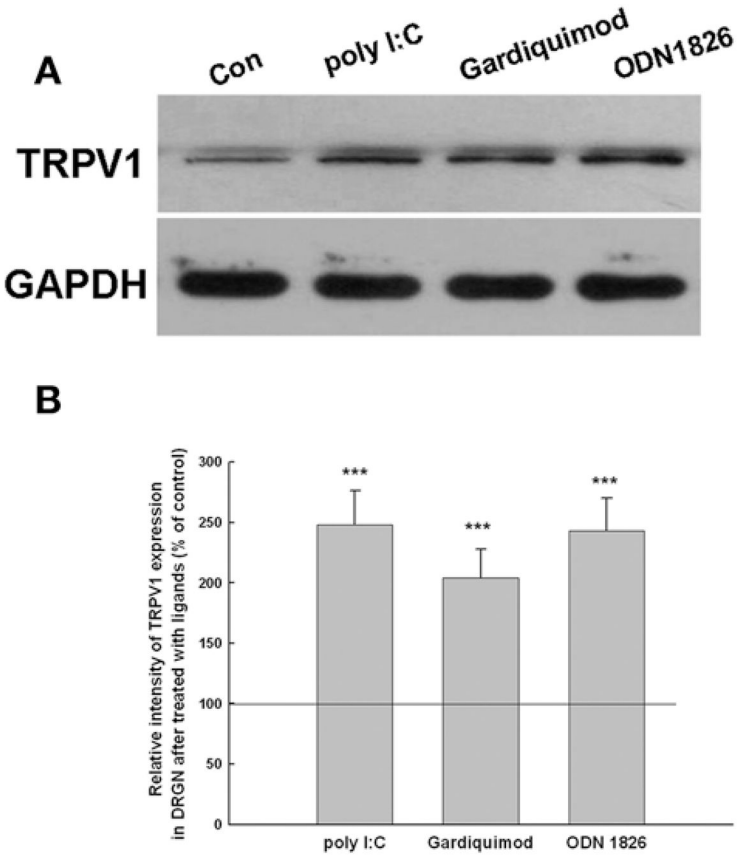

Fig. 6.

TRPV1 expression is increased on DRGNs stimulated with ligands for endosomal TLRs. (A) TRPV1 expression by DRGNs was detected by Western blot following stimulation by poly I:C (25 μg/ml), gardiquimod (3 μg/ml) or ODN 1826 (32 μg/ml) for 16 hrs. (B) Densitometry from the blots (% of control). Images densitometry were performed using ImageJ software. GAPDH was applied as internal control. One representative of more than three independent experiments is shown. ***$P < 0.001$ compared with control.

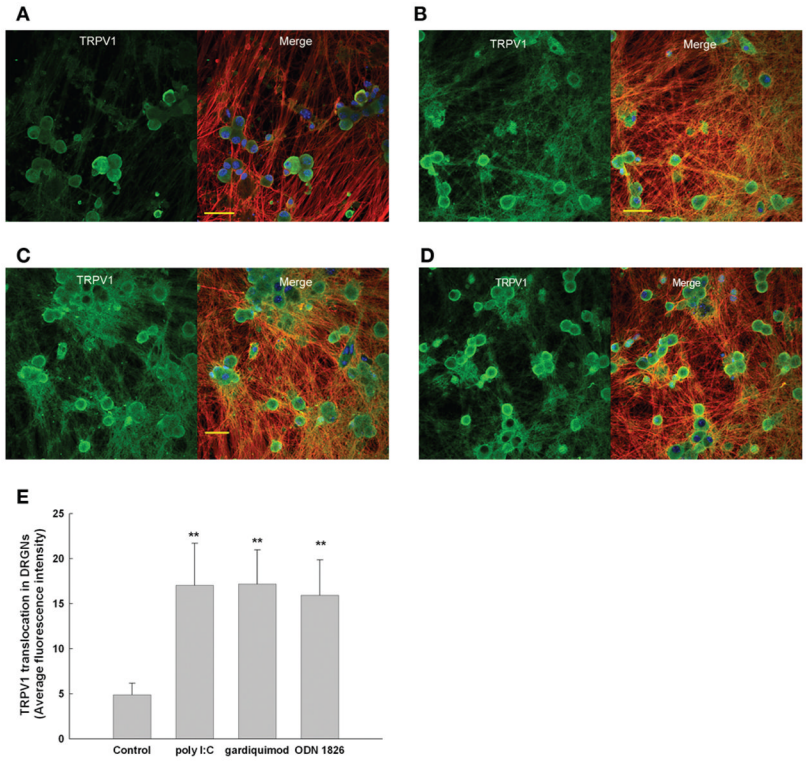

Fig. 7.

TRPV1 is expressed by DRGNs and relocates following TLR ligands stimulation. Confocal images of TRPV1 expressed by primary cultured mouse DRGNs are shown. DRGNs were stained with TRPV1 (green), neuron-specific beta-III tubulin (red) and DAPI (blue). Shown are monochrome images of the green fluorescence channel, and merged color images from all channels. (A) control, (B) poly I:C (25 μg/ml), (C) gardiquimod (3 μg/ml), and (D) ODN 1826 (32 μg/ml) stimulation for 16 hrs induced TRPV1 expression in DRGNs. Scale bars: 50 μm. (E) The average intensity of TRPV1 in the neuron surface and dendrites. Images intensity analysis was performed using ImageJ software. Statistical analysis was performed using Student's t test for two-group comparisons. $^{**}P < 0.01$ compared with control.

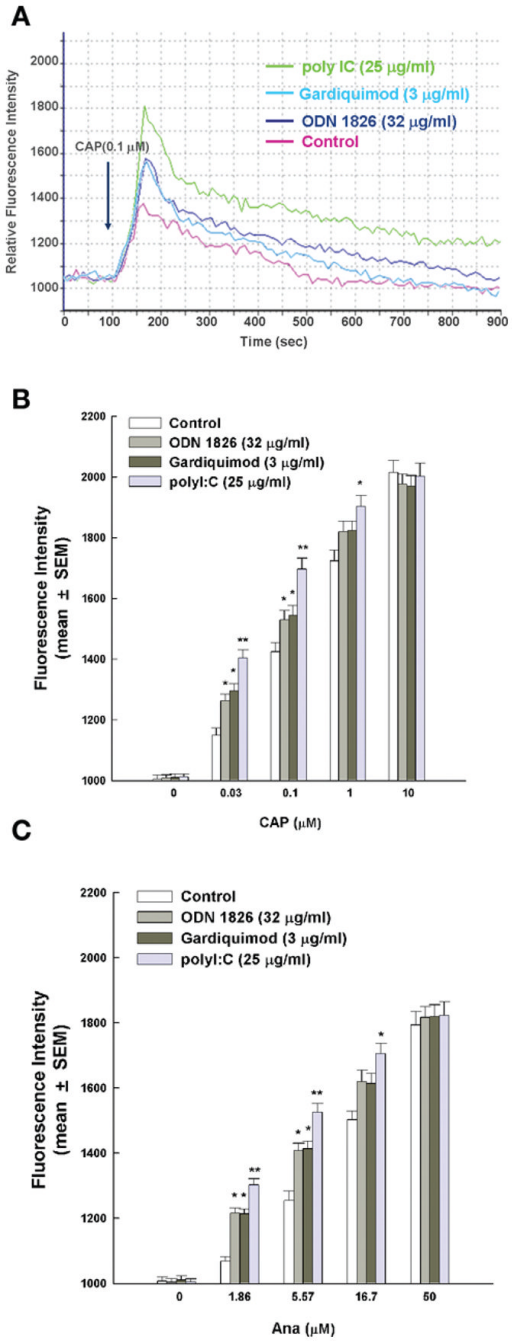

Fig. 8.

TLRs stimulation enhances the Ca^{2+} ion channel activity of TRPV1 in primary cultured DRGNs. (A) In DRGNs, CAP (0.1 μM) induced a greater Ca^{2+} flux in cells pretreated with poly I:C (25 μg/ml, green line), gardiquimod (3 μg/ml, light blue line) and ODN 1826 (32 μg/ml, dark blue line) for 16 hrs than without TLR ligands pretreatment (pink line). CAP was added at 90 s for 10 s. The curves were obtained from single cells of different treatment groups. Time in seconds is shown on the x-axis and relative fluorescent units are shown on the y-axis. (B) Dose-response curve of CAP-induced Ca^{2+} flux in the presence or absence of TLR ligands pretreatment. (C) Dose-response curve of Ana-induced Ca^{2+} influx in the presence or absence of TLR ligands pretreatment. Each bar represents the mean ± S.E.M.

(n=30). * $P < 0.05$, ** $P < 0.01$ compared with control. The data were analyzed by two-way ANOVA.

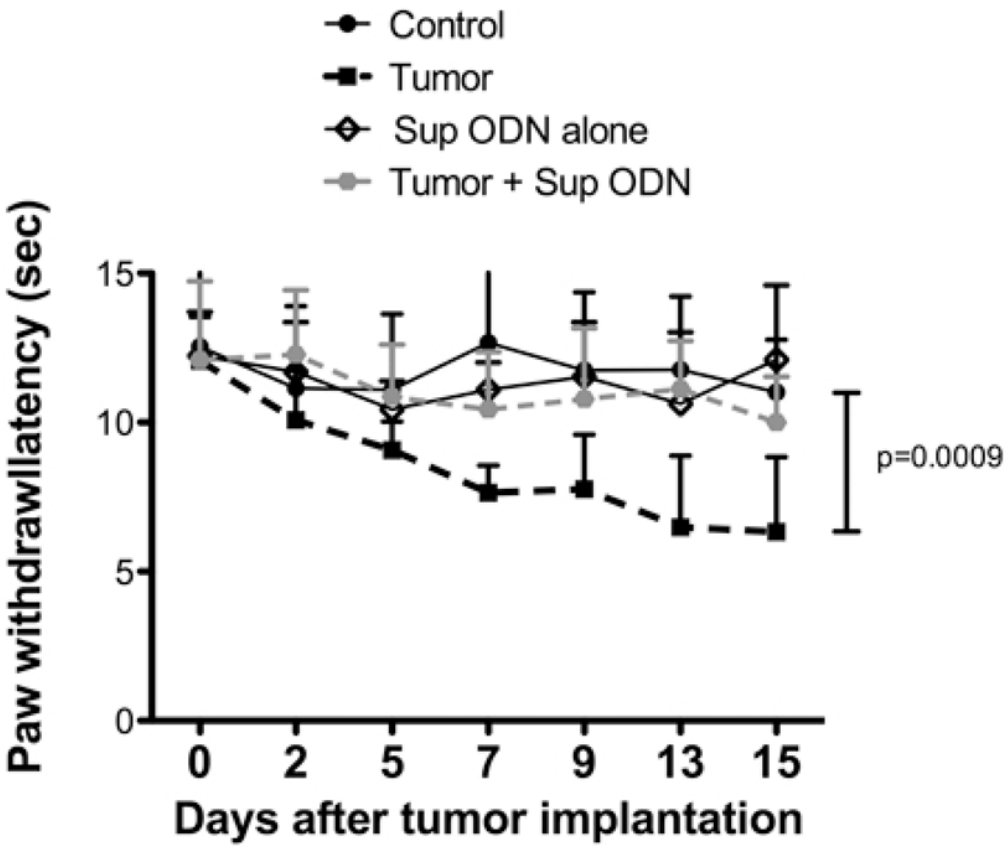

Fig. 9.

Suppressive ODN treatment blocks tumor-induced temperature sensitivity. The latency required for paw withdrawal from a 55°C hot plate was measured. Each point represents the mean time ± S.E.M (n=8). Comparisons are made between the naïve (Neg. Control) mice without S-180 tumor (shown with closed circles) and tumor-bearing mice, (shown with closed squares) or tumor-bearing mice and treated with 80 μg/mouse Sup ODN (shown with closed triangles). The probability of difference between Neg. Control and tumor-bearing mice (Tumor Control group, $P = 0.001$) or Sup ODN (80 μg/mouse Sup ODN group, $P = 0.06$) was determined using one-way ANOVA and Dunnett's test. The trends were graphed by linear regression and the one-way ANOVA post tested for linear trend ($P = 0.02$) supporting a dose response.

Table 1

(A) Fold changes in cytokines and chemokines mRNA levels and (B) protein concentrations after stimulated of DRGNs with TLRs ligands.

	Ligand	Cytokines and Chemokines			
		CCL5	**CXCL10**	**IL1-alpha**	**IL1-beta**
(A) mRNA fold increased compared to Control	polyI:C (25 μg/ml)	289.9±7.4*	73.8±5.4*	9.7±1.9*	10.9±1.9*
	Gardiquimod (3 μg/ml)	16.9±1.56*	7.4±0.35*	8.9±0.69*	10.4±1.7*
	ODN1826 (32 μg/ml)	9.1±0.69*	7.6±0.17*	6.4±1.7*	6.6±1.4*
(B) Protein concentration (pg/ml)	Control	16.6±2.9	193.9±58.3	0.6±0.17	1.2±0.34
	polyI:C (25 μg/ml)	1899.6±762.6*	26455.8±9714.8*	2.3±1.2*	7.8±2.9*
	Gardiquimod (3 μg/ml)	76.8±25.8	505.7±225.1	3.2±0.17*	2.8±0.52*
	ODN1826 (32 μg/ml)	25.0±5.2	410.0±206.0	1.6±0.34*	3.3±0.69*

DRG cultures were treated with TLRs ligands for 16 hrs. Total RNA was isolated from neurons by RNA isolation kit and reverse-transcribed into cDNA. Each PCR array for quantitative PCR reaction was carried out. The protein levels in supernatants of DRG cultures were determined by multiplex array. The results represent the mean ± SD Data for RNA array were analyzed by RT^2 Profiler PCR Array Data Analysis software (SABioscience). Statistical analysis for the protein levels were performed by Student's t test.

*$P<0.05$ compared with control n = 3.